Species-specific loss of genetic diversity and exposure of deleterious mutations following agricultural intensification

Zachary J. Nolen[1*], Patrycja Jamelska[1], Ana Sofia Torres Lara[1,2], Niklas Wahlberg[1], Anna Runemark[1]

[1] Department of Biology, Lund University, Lund, Sweden 22362
[2] Faculty 2 Biology/Chemistry, University of Bremen, Bremen, Germany 28359

*Corresponding author: Zachary J. Nolen

Email: zachary.nolen@biol.lu.se

Keywords: Conservation, agricultural intensification, inbreeding, genetic load, genomic erosion

Abstract

Agriculture driven land-use change is a major contributor to insect declines globally. As a result of population decline and subdivision, species lose genetic diversity, potentially reducing adaptive potential and increasing genetic load, reinforcing decline. We examine how genetic diversity has changed over the past century in three Polyommatinae butterfly species in Sweden, leveraging genome sequencing of specimens from museum collections. Based on 59 historical and 90 contemporary genomes, we document a 6% decline in genetic diversity in the strongly grassland associated *Cyaniris semiargus*, driven by increased population isolation. In contrast, generalist *Polyommatus icarus* and heathland specialist *Plebejus argus* have largely maintained genetic diversity and connectivity over the study period. The reduction in heterozygosity in *Cy. semiargus* results from increases in runs of homozygosity. Thus, loss of functional connectivity has led to inbreeding in *Cy. semiargus*, exposing greater proportions of weakly deleterious mutations and variants in highly conserved regions, in homozygous states. This realized burden likely reduces mean fitness and reinforces population decline, highlighting the need for well-connected grassland landscapes to maintain grassland specialist functional connectivity and genetic diversity. We complement these analyses with five additional Polyommatinae species, uncovering that warning- and alarm rates of decline are found in three of those, including in *Cy. semiargus*, currently listed as of least concern. This study highlights the necessity of incorporating genetic data into conservation planning, as threats from genetic erosion are not captured by census-based conservation assessments.

Introduction

Insect decline has received increased attention in recent years as reports uncover alarming declines in insect assemblages and biomass (1). Efforts to quantify this decline estimate that terrestrial insects are declining at an average rate of 11% per decade globally, with this trend being primarily driven by even stronger regional declines in Europe and North America (2). This stark decline is the result of a variety of anthropogenic pressures, primarily climate change and land use changes such as agricultural intensification and urbanization (1, 3–7). Intensive agricultural landscapes place a particularly strong pressure on grassland insect species (6), especially in Europe where formerly biodiverse semi-natural grasslands have been abandoned or converted into intensively cultivated land (8).

While these declines already have alarming implications for natural communities and ecosystem services in which insects play key roles, they can also leave insect populations with genetic challenges to long term persistence. Smaller populations are expected to lose genetic diversity faster than larger populations due to the stronger relative force of drift (9). This reduces their ability to adapt to changing environments (10, 11) and may allow partially recessive, weakly deleterious mutations to accumulate and become unmasked through inbreeding and weakened selection (12, 13). Such accumulation of weakly deleterious mutations increases the genetic load, classically defined as the reduction in population fitness from an optimum genotype (14). This, in turn, may reinforce demographic decline in a process referred to as mutational meltdown (15). An increasing number of studies even document that decline of genetic diversity and accumulation of deleterious mutations may continue after demographic recovery due to drift debt (16–19).

How to assess the threat genetic factors pose to natural populations is still an active area of research, with several genetic monitoring approaches being suggested and implemented (20–23). Interpretation of genetic diversity is complex, as it is influenced by a multitude of factors (24), such as ecology and life history (25), genomic architecture (26), and demographic trends over thousands to millions of years (27). Some empirical studies have shown that populations may persist despite low levels of genetic diversity (28, 29) and that relationships between genetic diversity and extinction risk are context dependent (30). Therefore, the value of neutral genetic diversity in conservation management has been subject to some debate (31–33).

As a means to control for factors that may make interpreting absolute estimates of genetic diversity challenging, measures that estimate the rate of genetic erosion have seen increasing focus in genetic monitoring. Programs in several countries use genetic metrics measured at multiple time points or that directly estimate ongoing genetic erosion (21, 34, 35). Examining decline directly rather than setting thresholds for absolute levels of genetic diversity enables identifying populations for which ‘low’ genetic diversity is likely to increase extinction risk. For instance, larger populations are expected to have higher

numbers of segregating deleterious mutations (36), making them more prone to inbreeding depression following population decline (12, 37, 38).

Temporal sampling is limited to estimating genetic erosion from the first sampled time point, even if genetic erosion could have begun several decades before this time point. To overcome this constraint, genomic resources from historic samples preserved in natural history museums can extend monitoring further back in time. The direct measures of pre- and early bottleneck genetic parameters museum samples provide are crucial to fully understand the extent and character of genetic decline (23). Comparisons with historical samples may even allow approximating changes in genetic load across bottlenecks by comparing counts of putatively deleterious mutations (12, 19, 23, 39–41). Such studies have the potential to identify populations that face reduced fitness from decline.

Here, we use museomics to address to what extent genetic diversity has been lost and functional connectivity reduced in grassland associated butterflies during the second wave of agricultural modernization in Sweden starting in the 1940s (42, 43). During this modernization, small farms were abandoned, and their associated semi-natural grasslands began to decline considerably (43). We examine three focal butterfly species in this landscape that vary in habitat specialization, ranging from grassland generalist to specialist, enabling us to examine if patterns of genetic decline are stronger in more specialized species, in line with expectations from greater demographic declines in specialist insect abundance compared to generalists (44–46). By comparing pairs of historical population samples collected in southern Sweden in the early 20th century with their contemporary counterparts, we document species-specific losses of genetic diversity and functional connectivity, and increased homozygosity of putatively deleterious mutations that is expected to have increased genetic load in the most specialized species. We further examine if loss of genetic diversity is reflected in current conservation status, by extending the dataset to include historical and modern individuals of five additional related butterfly species with Swedish Red List (47) conservation statuses ranging from least concern to critically endangered.

Results

We analyzed changes in genetic diversity, differentiation, and deleterious mutation burden in three focal Polyommatinae (Lepidoptera: Lycaenidae) butterfly species: *Polyommatus icarus,* a grassland generalist, *Plebejus argus*, a heathland specialist, and *Cyaniris semiargus*, a grassland specialist (Figure 1A). We generated whole genome resequencing data from pinned museum specimens from the entomological collections of the Biological Museum at Lund University (48) collected from 1917-1956 (Table S1; *N* = 28 - *Po. icarus*; 12 - *Pl. argus*; 14 - *Cy. semiargus*) in southern Sweden. These individuals were sampled as populations by grouping specimens generally collected at the same locality during the same year, and compared with WGS data from samples collected at corresponding localities in 2020-2023 by Nolen et al

(49) (Figure 1B; Table S1; *N* = 27 - *Po. icarus*; 29 - *Pl. argus*; 29 - *Cy. semiargus*). As DNA extracted from historical specimens is fragmented and subject to post-mortem DNA damage (50, 51) (Figure S1), we removed transitions from all analyses. As the shorter fragment size of historical samples can result in poor mapping of reads containing non-reference alleles, we constructed variation graphs for each reference genome containing high quality variants called in the modern samples. Mapping both sample types to these variation graphs reduced reference bias compared to aligning to the linear reference genome, as well as reduced the disparity in reference bias between historical and modern samples, especially when calling genotypes (Figure S2&3; Supplementary Methods). While this alignment method reduced reference bias in historical samples, it was not eliminated, and results should be considered with this in mind, especially for *Po. icarus* which exhibits the largest residual bias (Figure S2). Median sequencing depth was 6.4x (range = 2.2 to 16.7x) for historical samples and 19.3x (range = 7.0 to 56.7x; Table S1) for modern samples. To account for variation in sequencing depth, all analyses were performed with data subsampled to 6 to 8x sequencing depth.

Reduced genetic diversity and effective population size in Cy. semiargus

To assess if agricultural intensification and the associated reduction in semi-natural grassland habitat has resulted in reduced genetic diversity, we compared individual genome-wide heterozygosity of historical and modern samples within each species. Individual heterozygosity is significantly reduced in the specialist *Cy. semiargus* (percent difference: -6%; LMM: $P = 0.008$; Figure 1C; Table S2&3), but not in *Po. icarus* or *Pl. argus*. Population specific changes in genetic diversity estimated both from mean heterozygosity and nucleotide diversity (Table S4) suggest that genetic diversity has mostly been reduced in populations in Skåne, with < 1% change in Småland (Tables S5&6).

To understand the demographic patterns that may have led to these declines, we assessed changes in effective population size (N_e) over the past century using a linkage disequilibrium (LD) based method on the modern genomes. We find stable and very high effective population sizes in *Po. icarus* and fluctuating or only recently declined sizes in *Pl. argus*, in line with their maintenance of genetic diversity (Figure S4; Table S6). In *Cy. semargus*, we find that all populations in Skåne have gone through population declines in the past 30 generations, currently maintaining effective population sizes of 35 (SE Skåne), 202 (W Skåne), and 520 (E Skåne) (Figure S4; Table S6).

Reduced connectivity may drive loss of genetic diversity

While genetic diversity decline is an expected product of demographic decline, it can additionally be caused and accelerated by reductions in gene flow (52). We reveal reduced functional connectivity among modern *Cy. semiargus* populations, reflected in stronger contemporary population structure inferred from both genetic differentiation and clustering approaches. For population pairs represented in both modern and historical samplings, modern estimates of genetic differentiation (F_{ST}) in *Cy. semiargus* have increased from an average of 0.041 to 0.065, with the increase being largest between W Skåne and

Småland (Figure 1E; Table S7). Including population pairs in the modern sampling that are not represented in the historical, but that include similarly geographically separated populations, increases the average F_{ST} of modern *Cy. semiargus* pairs to 0.086. For *Po. icarus* and *Pl. argus*, average F_{ST} between pairs represented in both time periods has changed from 0.018 to 0.011 and 0.034 to 0.038 (Figure 1E; Table S7). When including additional modern pairs in *Pl. argus*, the modern average is slightly lower, 0.035, though this includes pairs at short distances that are not represented in historical pairs. Historical population pairs are sampled at different time points, with pairs including populations sampled up to 20 years apart (Table S7), which could inflate historical F_{ST} estimates.

Principal component analyses (PCAs) and admixture analyses also reveal stronger population structure in modern *Cy. semiargus* samples than historical (Figure 2A). Each modern population forms a distinct cluster in the specialized *Cy. semiargus*, with modern Småland samples clustering with their historical counterparts (Figure 2B). Historical samples from Western and Eastern Skåne cluster together in a separate cluster from the respective modern samples, highlighting that the stronger genetic structure found in modern samples is largely driven by isolation of populations in the agricultural landscapes within Sweden's southernmost province, Skåne (Figure 1D; Figure 2A&B; Figure S5). Populations of both *Po. icarus* and *Pl. argus* from Skåne separate from those sampled elsewhere in southern Sweden along the major axis of variation, with historical samples clustering with geographically proximal modern samples. Admixture analyses support only one genetic cluster in each of these species (Table S8), but the correlation of residuals suggest additional genetic clusters in *Pl. argus* (Figure S6), consistent with the PCA. This highlights that while genetic structure likely exists, the variation is too low for reliable clustering of samples at these sample sizes. We additionally find that historical and modern samples separate out on PC2 in *Po. icarus*, potentially an artifact of residual reference bias in historical samples of this species (Figure S2). The general pattern of historical populations clustering in the PCA with at least one geographically proximal modern populations suggests that historical samples are representative of ancestral populations to the modern ones.

Species-specific increases in inbreeding

To investigate changes in patterns of inbreeding, we estimated the inbreeding coefficient F_{RoH}, which is the proportion of the autosomal genome in runs of homozygosity (*RoH*) greater than a certain length (53), in our case 100kb, corresponding roughly to identical by descent tracts with shared ancestry in the past 200 generations (54). We found a significant increase in F_{RoH} from historical to modern *Cy. semiargus* samples (difference: 0.065, LMM: $P < 0.01$; Figure 1D; Table S9). Across species, the highest inbreeding coefficient for a historical sample is 0.031, with historical species averages all below 0.01 (Tables S2&9). In *Cy. semiargus*, modern samples have a maximum coefficient of 0.329 and an average coefficient of 0.073, an order of magnitude higher than the mean for historical samples. The majority of individual inbreeding coefficients were composed of runs of homozygosity >= 1.5 Mb in length (Figure 3A), corresponding to low effective population sizes in the past ~12 generations, in line with estimates of

recently low effective population size in our demographic analyses. In *Po. icarus* and *Pl. argus*, both modern and historical estimates of F_{RoH} are low with averages <= 0.01, with no evidence for a significant increase in these species (Table S9).

To assess how much increased inbreeding has contributed to decline in heterozygosity, we estimated heterozygosity adjusted by F_{RoH} per individual, which roughly estimates heterozygosity outside of *RoH.* Outside of *RoH*, heterozygosity in *Cy. semiargus* was not different between time periods (Figure S7), suggesting that recent increases in inbreeding drive reduced genetic diversity rather than erosion by drift. To assess if reductions in heterozygosity solely explained by increases in F_{RoH} matches theoretical expectations, we performed coalescent simulations parameterized on the recent demographic histories inferred from the modern genomic data, estimating heterozygosity and F_{RoH} for individuals sampled at time points corresponding to our modern and historical samplings. In all simulations, changes in heterozygosity were primarily explained by changes in F_{RoH}, lending support to our empirical estimates (Table S10). Additionally, for all simulated populations except for Småland *Cy. semiargus*, our empirically estimated ratios of modern/historical heterozygosity fell within predicted ranges, as did average modern F_{RoH} (Figure S8).

Increased homozygosity of weakly deleterious mutations in Cy. semiargus

Population decline and subdivision can increase the exposure of partially recessive, deleterious mutations to selection due to increased homozygosity, facilitating purging of strongly deleterious mutations (55–57). However, as populations decline and subdivide, selection weakens relative to drift, allowing partially recessive, weakly deleterious mutations to drift to higher frequencies and fix, increasing genetic load (13, 15, 58). Here, as a proxy for genetic load, we estimated deleterious mutation burden per individual using derived counts of putatively deleterious mutations (as in e.g. 19, 39, 41, 59, 60). Deleterious mutations were identified based off the functional annotation or the sequence conservation score of the position and divided into three categories: (I) missense, i.e. weakly deleterious; (II) loss of function (LoF), i.e. strongly deleterious; and (III) conserved, i.e. with high sequence conservation across Lycaenidae, presumed to be strongly deleterious. We partitioned burden into ‘total burden’, approximating load if mutations are primarily additive, and and ‘homozygous burden’, reflecting load if mutations are primarily recessive.

We find no evidence of changes in the total burden for any of the three mutation categories in *Po. icarus* or *Cy. semiargus*. However, in *Pl. argus*, total burden at missense positions is reduced (LMM: $P < 0.001$; Figure 3B; Table S10), consistent with purging of weakly deleterious mutations. This reduction does not appear to be driven by differences in sample quality, as there is no significant change in any other mutation category or in the derived count at either intergenic or synonymous genic positions (Table S11). Homozygous deleterious burden has increased at conserved positions in *Pl. argus* (LMM: $P = 0.006$; Figure 3B; Table S10) and missense and conserved positions in *Cy. semiargus* (LMM: $P = 0.002$ and 0.006; Figure 3C; Table S10), but not changed over time in *Po. icarus*. There is no change in homozygous burden at LoF positions over time in any species. *Cyaniris semiargus* individuals with higher

inbreeding coefficients also had higher homozygous burden across all categories of deleterious mutations (LM: R^2 = 0.83, 0.40, 0.76 for missense, LoF, and conserved positions, respectively; Figure S9). There is also a weaker increase of total burden with inbreeding coefficient at LoF and conserved positions (LM: R^2 = 0.12, 0.12, respectively).

Genetic diversity indicators

We utilized the genetic diversity indicator thresholds outlined by Andersson et al. (20) to determine if current conservation status relates to the rate of genetic erosion. These thresholds suggest categorizations of 'Acceptable', 'Warning', and 'Alarm' rates of genetic erosion, reflecting >=95%, 75-94%, and <75% retention of genetic diversity over 100 years, respectively. Based on changes in mean population heterozygosity and nucleotide diversity, populations of all three species largely fall in the 'Acceptable' category, with the exception of *Cy. semiargus* in Southeast and Western Skåne, which fall into 'Warning' category (Figure 4; Tables S5&6). The same indicator framework in Sweden categorizes effective population sizes >= 500 as 'Acceptable', 51 - 499 as 'Warning', and <= 50 as 'Alarm' (20, 61). Under this indicator, all *Po. icarus* and *Pl. argus* populations and Småland *Cy. semiargus* would be classed as 'Acceptable'. The low effective population sizes in Skåne for *Cy. semiargus* would place Eastern Skåne as 'Acceptable', but bordering on 'Warning', Western Skåne as 'Warning', and Southeastern Skåne as 'Alarm' (Table S6).

To assess genetic erosion across a broader range of grassland butterfly species, we supplemented the focal dataset with whole genome data for historical-modern pairs of five additional species of Polyommatinae butterfly (Table S1). We assessed if the conservation status of these species, ranging from of 'Least Concern' to 'Critically Endangered' (47) (Table S12) are associated with genetic erosion. As these additional species were pairs of individuals rather than population samples, we reassessed the focal three species, comparing all historical-modern individual pairs for each population. We find that 'Least Concern' species largely show 'Acceptable' changes in genetic diversity, with the exception of Southeastern and Western Skåne *Cy. semiargus*, which fall into the 'Warning' category. Of the Red Listed species, *Cupido minimus* ('Near Threatened') falls into the 'Acceptable' category, *Plebejus argyrognomon* ('Critically Endangered') into 'Warning', and *Scolitantides orion* ('Endangered') into 'Alarm' (Figure 4; Table S6). Results from our focal species illustrate that estimates from single individuals are challenging to interpret, as estimates can vary considerably depending on the individual pair (Figure 4).

Discussion

Our analyses of 59 historical and 90 modern genomes uncover a decline in genetic diversity in the specialist grassland butterfly *Cyaniris semiargus* over the past century. The previously connected populations of this species in southern Sweden have become isolated into distinct genetic clusters following agricultural intensification. Increased rates of inbreeding have unmasked a portion of the weakly

deleterious burden in *Cy. semiargus* and *Pl. argus*, potentially depressing individual and mean fitness. This constrasts to the generalist *Polyommatus icarus*, where we detect minimal changes in genetic diversity, inbreeding, and genetic differentiation over the focal period. All three species share a status of 'Least Concern' in Sweden, highlighting that assessing genetic erosion can identify risks to species and populations not captured by census-based conservation assessments.

We uncover a loss of population connectivity in *Cy. semiargus*, evidenced by increased population structure in the clustering analysis and higher genetic differentiation among modern populations. The historically lower levels of genetic differentiation across southern Sweden in *Cy. semiargus* highlights that currently isolated populations in Skåne are subsets of a historically well-connected metapopulation. Moreover, the similarly high estimates of historical effective population size in West- and Eastern Skåne likely provide an independent line of evidence supporting this interpretation. Their concurrent abrupt declines may reflect the cessation of gene flow, shifting effective size estimates from those of the metapopulation to estimates for each subpopulation. This pattern is consistent with theoretical expectations of high genetic diversity being maintained by even low levels of gene flow (62, 63), as documented in another Lycaenid butterfly (64). Hence, concerns about genetic rescue (65) wiping out locally adapted ancestry (66, 67) are not likely to be relevant for these and other grassland associated insects in regions with historically abundant habitat.

In the specialist *Cy. semiargus* we document an on average 6% reduction in heterozygosity. We uncover that this reduction largely results from the accumulation of runs of homozygosity, resulting from recent population isolation and inbreeding, as expected from our simulations of recent demographic decline. In contrast, for *Po. icarus* and *Pl. argus*, analyses of population structure and genetic differentiation are consistent with gene flow maintaining functional connectivity, as no significant increases in population subdivision are observed. Consistently, levels of heterozygosity remain stable and inbreeding remains low in these species. However, temporal changes in effective population size suggest that *Pl. argus* has experienced very recent declines, though not to sizes as low as *Cy. semiargus*. Hence, there is a possibility that there have been recent reductions in gene flow in this species despite stable estimates of differentiation, as population differentiation accumulates over time, lagging behind reductions in gene flow (68, 69).

Understanding to what extent genetic diversity decline, resulting from habitat loss and isolation, reduces the fitness of individuals and populations is crucial for determining conservation priorities. To approximate reductions in fitness without having direct estimates available, we quantified deleterious mutation burden as a proxy for genetic load (70). Dominance coefficients of the estimated deleterious burden are key for interpreting its effects on fitness and prospects of purging. Theoretical predictions (55–57) and empirical evidence (19, 59, 71–74) suggest that population decline can increase exposure of partially recessive, deleterious mutations to selection, reducing their frequency. Dominance coefficients are generally lower for more deleterious segregating deleterious mutations (75), whereas dominance coefficients for weakly

deleterious mutations are estimated to be around 0.2-0.25 (76, 77), which would suggest more efficient purging of more deleterious mutations. Weakly deleterious mutations are less likely to be efficiently purged in small populations than strongly deleterious ones (55, 57), often requiring low dominance coefficients for purging to be effective (55). A recent model does, however, suggest that dominance coefficients may commonly be close to zero for even weakly deleterious mutations (78). Interestingly, evidence of purging was only observed for weakly deleterious burden from missense mutations in *Pl. argus*, which decreased ~4%. A similar pattern of purging of a portion of the weakly deleterious burden, attributed to mutations with high recessivity, has been observed in the Iberian Lynx (59). The modest purging in *Pl. argus* should nevertheless be considered cautiously, as it could be an artifact of differential sampling of historical and modern populations, or differences in in sample quality, though we find no evidence of a similar decline in the derived count at intergenic or synonymous positions as expected if it would be an artifact of sample quality. Our demographic inferences for *Pl. argus* suggest that while no population has reached very small size, some have experienced recent fluctuations or reductions in effective population size. Fluctuations at relatively large population sizes may have facilitated mild purging of a portion of the most recessive weakly deleterious burden, as predicted from models of deleterious mutation count during a bottleneck (59).

Translating estimates of deleterious mutation burden to fitness effects remains an empirical challenge. Jointly, the partial recessivity of segregating deleterious mutations (76–78) and the frequency of inbreeding depression in outcrossing organisms (58, 66, 79, 80) suggest that negative fitness effects for deleterious mutations are primarily realized when exposed in homozygous state. Based on these patterns, genetic load is suggested to be more closely approximated by the homozygous, rather than the total, deleterious burden (60). In the grassland specialist *Cy. semiargus*, deleterious burden has increased in homozygosity at both missense and conserved variants, but not LoF variants. As both burden at missense and conserved variants is strongly associated with the inbreeding coefficient, this can be interpreted as unmasking of the inbreeding load present in the historical populations (12, 66, 81). In *Pl. argus*, however, homozygous burden at conserved variants has increased in frequency, even if no increase in inbreeding coefficient was observed. Understanding the link between measures of deleterious mutation burden and fitness based estimates of load is important for assessing the validity of assumptions underlying estimates of burden and interpreting the effects of observed changes. For instance, the functional effect-based estimates used to classify missense and LoF variants are reliant upon the accuracy of underlying gene model and the inference of ancestral allelic states. Estimates of burden using sequence conservation scores also assume more conserved regions are more functionally important (12, 82). Our findings for conserved sites more closely resemble those of missense than LoF mutations. While mutations at conserved sites are expected to have relatively strong effects (12, 82), sequences conservation scores have been shown to have a limited ability to distinguish between weakly and strongly deleterious mutations (83, 84). In addition, GERP scores depend on estimates of the rate of neutral evolution, approximating the rejected substitution rate. Our GERP scores are based on a time tree

(similar to 39, 40, 73, 83) and hence differ from scores estimated based on neutral rates (e.g. 85). However, our identification of conserved sites should be robust for within-species comparisons of deleterious burden, as they represent the most conserved variants in our datasets. Despite these caveats, our estimates of deleterious burden are consistent with expectations under patterns of population decline for *Cy. semiargus*. Increased homozygosity of burden at missense and conserved positions in *Cy. semiargus* highlights that populations may now persist at small enough sizes that inbreeding depression poses an additional threat to persistence. While our estimates of deleterious burden include variants fixed within single populations, almost none of these deleterious variants are fixed across all populations. This suggests that translocation and restoration of functional connectivity would facilitate genetic rescue (86, 87).

Estimates of deleterious burden remain only a rough approximation of the true genetic load, and an increase in the homozygous burden does not necessarily indicate reduced fitness. For instance, if the portion of weakly deleterious mutations that have increased in homozygosity tend to be more additive than recessive, fitness will not be reduced considerably if the total burden remains unchanged. It is therefore paramount to determine the relationship between estimates of deleterious burden, fitness and extinction risk. A negative relationship between heterozygosity and extinction risk has been documented in the Glanville fritillary butterfly (*Melitaea cinxia*) for small, isolated, recently declined populations (30). An increased homozygous deleterious burden as we observe in small, isolated, recently declined populations of *Cy. semiargus* likely could cause the fitness consequences observed in isolated *M. cinxia* populations (30, 88, 89). Systems such as this, where joint estimation of fitness and deleterious mutation burden is possible, are key to fully understanding how well different genomic measures of mutation burden approximate genetic load, knowledge crucial for assessing conservation status of wild populations.

None of the three focal species are currently demographically declining at a rate to qualify for the Swedish Red List based on census estimates. Systematic monitoring in Sweden from 2010-2023 reveal declines in both *Po. icarus* and *Cy. semiargus*, while *Pl. argus* appears to have stabilized (90). In *Cy. semiargus*, increased homozygous burden could already be contributing to its demographic decline. Our findings illustrate the importance of incorporating genetic monitoring into conservation assessment (91, 92) to identify genetic erosion before it substantially increases genetic load. Temporal monitoring with historical samples provides an opportunity to detect species facing recent declines in genetic diversity, separating them from those with longer term low genetic diversity (23). Using this approach on several species of Polyommatinae blues in southern Sweden, we find that genetic diversity is maintained in five of eight species. In addition to a ‘Warning’ categorization for *Cy. semiargus*, we uncover ‘Warning’ and ‘Alarm’ level classifications for two endangered grassland specialists, *Pl. argyrognomon* and *Sc. orion*, respectively. In all three species, reduced heterozygosity largely stems from increases in inbreeding. Measures of runs of homozygosity, combined with estimates of deleterious burden thus provide a promising way to assess genetic conservation concerns in the wild (19, 93). Estimates of both runs of

homozygosity and deleterious burden rely on the availability of high quality reference genomes and annotations, underscoring the importance of generating high quality reference genomes for conservation (94).

In conclusion, we document an inbreeding driven erosion of genetic diversity in some declining specialist grassland butterflies in southern Sweden. While census size based estimates of demographic declines largely inform current conservation status of these species, we show that these are insufficient to capture population isolation and resulting inbreeding, highlighting the value of genetic monitoring of wild insects to prevent extirpation and extinction. *Cyaniris semiargus*, a once widespread species in Sweden, provides a strong example of this, now persisting in segmented populations with increased rates of inbreeding and homozygosity of deleterious burden. Our findings suggest that prompt restoration of grassland connectivity in agricultural regions is needed to restore and maintain gene flow and reduce the risk of local extirpation of specialist grassland butterflies.

Materials and Methods

Study System and Sampling

To assess changes in genetic diversity, differentiation, inbreeding, and deleterious burden, we compared modern and historical genomes from three focal blue butterfly species (Polyommatinae), *Polyommatus icarus*, *Plebejus argus*, and *Cyaniris semiargus* (Figure 1A). These species vary in habitat specialization, being grassland generalist, heathland specialist, and grassland specialist, respectively. We used previously generated population-level genetic data (49) for the modern genomes. For the historical genomes, we selected pinned specimens from the entomological collections of the Biological Museum, Lund University (48) sampled between 1917-1956 in roughly the same geographic area as the modern samples. For each historical locality, we selected 4-11 specimens sampled in the same year to estimate population-level metrics. The historical and modern population-level pairs were sampled in four broad geographic areas: I) Western and II) Eastern Skåne, III) Småland, and IV) Öland (Figure 1B), with historical localities ranging approximately 12-40km from their modern counterparts. This resulted in three historical-modern population pairs for *Po. icarus* and two for *Pl. argus*. For *Cy. semiargus*, we included three pairs and an additional comparison of a modern Southeastern Skåne population with the historical Eastern Skåne population. For *Pl. argus*, only one historical specimen was available from Western and Eastern Skåne, respectively, and these were compared to the closest modern populations in individual-level analyses only.

To more broadly assess the variation in rates of genetic decline in Polyommatinae of differing conservation statuses, we sampled historical and modern individuals of five additional species: *Agriades optilete, Aricia agestis, Cupido minimus, Plebejus argyrognomon* and *Scolitantides orion.* Modern specimens of *Ag. optilete, Ar. agestis,* and *Cu. minimus* were collected across the same geographic

regions as the focal species in 2021 (Table S1). A pinned specimen used as the modern sample of *Sc. orion* was collected in 2016 in Södermanland, and donated to this study by Håkan Elmqvist. Legs from a pinned speciemen of *Pl. argyrognomon*, collected in 2003 in Western Skåne, were donated by Göran Engqvist and used as the modern sample for this species. Historical samples for these five species were selected to be proximal to the modern specimen sampling locality with collection dates ranging from 1939-1967, all provided as pinned specimens from the entomological collections of the Biological Museum, Lund University (48).

DNA Extraction and Sequencing

DNA from fresh specimens was extracted and sequenced following Nolen et al (49). We extracted DNA and prepared sequencing libraries from pinned museum specimens in a facility dedicated to historical DNA processing at Lund University, following the protocol described by Twort et al (95). Libraries prepared for pinned specimens were pooled into two equimolar pools containing 37-38 libraries each, sequencing each pool on a single NovaSeq 6000 S4 lane. DNA was extracted from the abdomens or legs of male specimens without homogenization to preserve anatomical structures.

Sequence Processing

Sequence processing and analyses were largely performed using Snakemake v8.25.5 (96), incorporating and extending the PopGLen v0.4.2 (97) workflow. We trimmed raw sequencing reads using fastp v0.23.4 (98) with default settings, additionally collapsing overlapping read pairs in historical samples, discarding those with less than 30bp overlap. As historical DNA is expected to be fragmented, mapping can be biased towards reads containing the reference allele. We investigated two potential alignment options to reduce this impact: (I) BWA aln (99) with relaxed parameters, as is used in the majority of historical DNA studies, and (II) alignment to a variation graph incorporating known alternative variants from the modern samples, which has been shown to reduce reference biases when mapping short fragments (100). As we found that mapping to the variation graph reduced the amount of reference bias in the historical samples (Figure S2&3), we performed all analyses with both modern and historical samples aligned to the species-specific variation graphs. Detailed methods of the processing for this comparison and the final alignment method are available in the Supplementary Methods, with a brief outline of the final method here.

To construct variation graphs for each species, we first aligned the trimmed, paired-end modern reads to the respective reference genome (Table S12) (101–103) using BWA mem v0.7.17 (104), removed duplicates using Picard v2.27 (105), and realigned around indels using the GATK (106). We called genotypes in these samples using the BCFtools multi-allelic caller v1.21 (107) and constructed a variation graph from these variants and the linear reference genome using vg v1.63.1 (108). To produce the final alignments we mapped modern and historical samples to the variant graph using vg with default settings, additionally setting -k 15 for historical samples as recommended by Martiniano et al. (100). We removed

duplicates with Picard and dedup v0.12.8 (109) for modern and historical samples, respectively, and clipped overlapping read pairs using BamUtil v1.0.15 (110). We estimated post-mortem DNA damage in historical samples using DamageProfiler v1.1 (111).

Genotype calling and filtering

To account for variation in sequencing depth, we subsampled all individuals to a mean depth of 6x using Samtools v1.20 (107). We excluded individuals with a mean coverage of less than 5x from genotype calling. We implemented a sites based filtering scheme (see Supplementary Methods) and called genotypes for each species jointly across samples using the BCFtools multi-allelic caller at sites passing the species filter sets (Table S13), including reads with minimum mapping and base qualities of 30 and 20, respectively. We filtered to biallelic and invariant positions, excluding those within 5bp of indels or a variant quality less than 30. We set genotypes with a depth less than 6 and heterozygous genotypes with one allele supported by less than 20% of the reads to missing. We removed transition positions across all samples and filtered out positions with more than 40% missing data in either the historical or modern sample subsets.

Heterozygosity, nucleotide diversity, and genetic differentiation

We estimated individual genome-wide heterozygosity for all samples from the called genotypes by dividing the count of heterozygous calls by the total count of called genotypes, including invariant sites. We estimated nucleotide diversity using Pixy v2.0.0.beta2 (112), which utilizes a sample-size weighted calculation. Nucleotide diversity estimates in these populations are robust to low (N = 4) sample size (49), and so we include estimates for all populations with multiple individuals. We estimated this summary statistic in 50kb non-overlapping windows for populations grouped by sampling locality, estimating the genome-wide mean across windows, and confidence intervals from 10,000 bootstraps, resampling windows with replacement. We estimated genetic differentiation using pairwise population F_{ST} with Pixy on the same windows with the Hudson estimator (113), which is robust to small and variable sample sizes (114). We estimated mean F_{ST} and confidence intervals with the same approach as nucleotide diversity.

Relatedness

As analyses of population structure can be sensitive to the presence of close relatives in the dataset, we estimated pairwise relatedness between all samples within each species dataset. We utilized the IBSrelate SFS-based method (115), as implemented in NGSrelate (116), to estimate R0, R1, and KING-robust kinship coefficients (117) for all pairs of individuals in the dataset. For input, we generated a Beagle file for each focal species dataset, using all sampled individuals, but subsampling individuals with higher coverage to 8X to reduce the influence of the large variation in coverage in our modern samples. We estimated genotype likelihoods in ANGSD v0.940 (118) using the GATK model from reads with a mapping quality >= 30, base quality >= 20, at positions with a minimum depth of three that passed

species-specific site filters. We called SNPs with a p-value < 1e-6, a minor allele frequency >= 0.05, and with data in at least 90% of the individuals.

Population Structure

We explored population structure using principal component analysis (PCA) as implemented in PCAngsd v1.10 (119). To obtain independent sites for population structure analyses, we estimated linkage disequilibrium in the Beagle file from the relatedness analyses using ngsLD v1.2.0 (120) and pruned SNPs using prune_graph (https://github.com/fgvieira/prune_graph; v0.3.2), assuming independence of SNPs >50kb apart and with a coefficient of correlation (r^2) < 0.1. We removed one individual from each pair of third-degree or closer relatives in the dataset (expected KING-kinship coefficient >= 0.0625; Table S14) before running the PCA.

We formally tested for population structure using admixture analyses for 1-8 ancestral clusters (K) using the pruned, relative removed Beagle file in NGSadmix v33 (121). We performed at least 20 replicate runs for each value of K, up to 100 total runs, stopping if the three highest likelihood replicates converged within 2 log-likelihood units of each other. The 'best-fit' value for K was then determined to be the highest K for which replicates met this convergence criteria, following Pečnerová et al (122). We further assessed the model fit for each value of K using evalAdmix v0.961 (123).

Runs of Homozygosity

We assessed rates of recent and background inbreeding by estimating the inbreeding coefficient F_{RoH}, the proportion of the autosomal genome existing in runs of homozygosity over a specified length, incorporating runs of homozygosity >100kb in our estimates of F_{RoH}. Per individual runs of homozygosity were estimated using BCFtools/RoH v1.19 (124). We set a constant species-specific recombination rate, assuming 50 centimorgans per autosomal chromosome as in Mackintosh et al [(26)] (Table S12), and ran the analysis on genotype calls at variable sites, setting the PL of unseen genotypes set to 30. To ensure F_{RoH} estimates were inferred equivalently in species with population and individual level sampling, we did not estimate allele frequencies, instead using a default minor allele frequency of 0.4 and ignored homozygous reference positions, as including these can inflate estimates of F_{RoH} based on our testing (Figure S10). We calculated F_{RoH} for each individual by dividing the cumulative length of runs of homozygosity by the total length of the autosomes.

Recent demography and coalescent simulations of heterozygosity loss

To infer timing and magnitude of demographic declines that may contribute to reduced genetic diversity, we inferred changes in effective population size over the past 100 years from the modern samples using the linkage disequilibrium-based approach implemented in GONE (125). We inferred these histories in modern samples by sampling locality, as this method performs best when input samples do not have additional genetic substructure (126). We performed this analysis on the called modern variants used to construct the variation graphs, which included transitions. As we observed a frequent sudden drop in the

most recent four generations in most of the GONE analyses, we visualized trajectories both including and excluding these generations (Figure S4).

To assess if our empirical estimates of heterozygosity decline and accumulation of runs of homozygosity fell within expected ranges for the characterized demographic changes, we performed coalescent simulations using Slendr (127) with the msprime (128) backend. For each modern locality with a paired historical locality, we constructed demographic models that followed size changes inferred for the most recent 100 generations in the GONE analyses. As most sampled populations showed a roughly constant historical size by this time point (Figure S4), we set the ancestral size to that of generation 100. For localities where we inferred a constant history of very large size (>100,000), we modeled a simple constant size model with N = 100,000. Due to the aforementioned sharp drop in the most recent four generations, we set these generations in the model to the estimate of generation five. For each sampled locality, we ran 100 replicate simulations of a single, 10 Mb chromosome with a recombination rate corresponding to 50cM (26) and a mutation rate of 2.9e-8 (129). At time points corresponding to the collection of the historical samples for a given locality and the most recent generation, we sampled 100 individuals from each simulation and calculated mean heterozygosity, F_{RoH}, and heterozygosity outside of *RoH* to infer a range of expected values to compare our empirical estimates to.

Deleterious mutation burden

As proxies for genetic load, we estimated the burden of deleterious mutations per individual using the count of derived alleles with putatively deleterious consequences. We inferred these consequences using two complementary methods, one based on gene annotations to infer functional effects (130) and the other identifying positions with high sequence conservation (131). As variants were called across the combined historical and modern sample set for each species, alleles that are fixed within one time category, but variable or fixed for the opposing allele in the other, are included.

To identify which alleles were likely ancestral, we co-inferred ancestral states and sequence conservation scores using the GenErode pipeline v0.6.2 (132), which estimates Genomic Evolutionary Rate Profiling (GERP) scores (82) from a set of outgroup species assemblies. We utilized 24 Lycaenidae chromosome-level genomes from distinct genera (Table S15) (101–103, 133–136) as outgroups, modifying the default fragment size for GenErode's alignment step from 35 to 100bp, and using divergence times estimated with TimeTree 5 (137). We then subset the variable sites to include only those with GERP > 0 and where the ancestral allele matched the reference to avoid underestimating derived counts in historical samples.

We identified deleterious mutations based on functional effects using the genome annotations provided by the Darwin Tree of Life Project (https://projects.ensembl.org/darwin-tree-of-life/). We assigned impacts to each variant using Ensembl's Variant Effect Predictor (VEP) v112.0 (130). VEP categorizes variants into four classes: 'High', 'Moderate', 'Low', or 'Modifier', which largely correspond to loss of function, missense, synonymous, and intergenic variants. We forced VEP to pick one effect per variant, using the

default selection order (130). To identify conserved positions we selected the top 1% of GERP scores as the most conserved positions using the get_gerp_score_percentile.py script included with GenErode. We inferred deleterious burden at positions inferred as loss of function ('High' impact), missense ('Moderate' impact), or conserved based on GERP scores, using the derived allele count at these positions. Total deleterious burden is the total derived allele count of a variant category per 1000 called genotypes. Homozygous deleterious burden is the homozygous derived allele count per 1000 called genotypes. We additionally estimated these counts at synonymous ('low' impact) and intergenic positions to assess biases in derived counts across sample types.

Categorizing rates of genetic decline

To assess the changes in genetic diversity in a framework developed for conservation focused genetic monitoring, we used the indicator thresholds suggested by Andersson et al (20), which are based upon indicators applied for national use in Sweden (61). Using these thresholds, genetic decline within populations is measured as the amount of genetic diversity retained over a period of 100 years, assuming a constant rate of change. Three threat categories are suggested: retention >=95% is considered 'Acceptable', 75-94% as 'Warning', and <75% as 'Alarm'. We estimated the predicted retention of genetic diversity over 100 years for each population using individual heterozygosity and nucleotide diversity. Genetic diversity retention per year was estimated using the following equation:

$$e^{\frac{ln(H_{mod}/H_{hist})}{Y_{mod}-Y_{hist}}}$$

where H is the estimate of genetic diversity for a given sample/population and Y is the sampling year for that sample/population. We estimated this metric for nucleotide diversity in the focal species using population mean estimates. For individual heterozygosity, we estimated this metric using population means in the focal species and using all pairwise comparisons of historical and modern individuals in both focal and supplemental species. For the effective population size indicator we utilized the estimate of effective population size at generation five in the GONE analyses.

Acknowledgements

We would like to thank Melina Eberhagen, Amanda Görnerup, Kajsa Svensson, Aske Brydegaard Runemark, and Mikkel Brydegaard for assistance with collecting butterflies, Håkan Elmqvist for providing pinned *S. orion* specimen, Göran Engqvist for providing tissue from the pinned specimen of *Pl. argyrognomon*, Emma Kärrnäs and Isolde van Riemsdijk for assistance with DNA extractions, Jadranka Rota for assistance with the entomological collections of the Biological Museum, Lund University (https://doi.org/10.15468/dahk2a), Verena Kutschera and the Swedish Bioinformatics Advisory Program for advice regarding the bioinformatic analyses, Anna Penna for comments on the manuscript, and Isolde van Riemsdijk, Rachel Steward, Kalle Tunström, Simon Jacobsen Ellestrand, Colin Olito, Magne Friberg,

Mikkel Skovrind, and Carolina Pacheco for helpful discussions regarding the study species, methods and interpretations. We would like to thank Project Psyche and the Darwin Tree of Life project for generating and providing the reference genomes that made these analyses possible. We acknowledge support from the National Genomics Infrastructure in Genomics Production Stockholm funded by Science for Life Laboratory, the Knut and Alice Wallenberg Foundation and the Swedish Research Council. Computational resources were provided by the National Academic Infrastructure for Supercomputing in Sweden (NAISS) and the Swedish National Infrastructure for Computing (SNIC) at UPPMAX partially funded by the Swedish Research Council through grant agreements no. 2022-06725 and no. 2018-05973. This work was supported by grants from “Biodiversity and Ecosystem services in a Changing Climate” (BECC), the Foundation Oscar och Lili Lamms Minne, and the Swedish Research Council for Sustainable Development (grant 2021-01163) to AR and the Jörgen Lindström’s Foundation to ZJN.

Data Availability Statement

The genetic data that support these findings will be made available upon publication at NCBI in BioProjects PRJNA1068054 (focal species, modern) & PRJNA1168917 (focal species, historical; additional species). Bioinformatic workflow configurations, extensions, and resources specific to this study are available at https://github.com/zjnolen/polyommatini-temporal-genomics and archived at https://doi.org/10.5281/zenodo.13902816.

Author Contributions

Zachary J. Nolen: Conceptualization, Methodology, Formal analysis, Investigation (Lead), Data curation, Writing – original draft, Visualization, Funding acquisition. **Patrycja Jamelska**: Investigation (Supporting). **Ana Sofía Torres Lara**: Investigation (Supporting), Writing - review & editing. **Niklas Wahlberg**: Methodology, Writing – review & editing, Supervision. **Anna Runemark**: Conceptualization, Methodology, Writing – review & editing, Supervision, Funding acquisition.

References

1. D. L. Wagner, E. M. Grames, M. L. Forister, M. R. Berenbaum, D. Stopak, Insect decline in the anthropocene: Death by a thousand cuts. *Proceedings of the National Academy of Sciences* **118**, e2023989118 (2021).

2. R. van Klink, *et al.*, Meta-analysis reveals declines in terrestrial but increases in freshwater insect abundances. *Science* **368**, 417–420 (2020).

3. R. Dirzo, *et al.*, Defaunation in the Anthropocene. *Science* **345**, 401–406 (2014).

4. C. A. Halsch, *et al.*, Insects and recent climate change. *Proceedings of the National Academy of Sciences* **118**, e2002543117 (2021).

5. P. H. Raven, D. L. Wagner, Agricultural intensification and climate change are rapidly decreasing insect biodiversity. *Proceedings of the National Academy of Sciences* **118**, e2002548117 (2021).

6. S. Seibold, *et al.*, Arthropod decline in grasslands and forests is associated with landscape-level drivers. *Nature* **574**, 671–674 (2019).

7. D. H. Boyes, D. M. Evans, R. Fox, M. S. Parsons, M. J. O. Pocock, Is light pollution driving moth population declines? A review of causal mechanisms across the life cycle. *Insect Conservation and Diversity* **14**, 167–187 (2021).

8. J. R. Shipley, *et al.*, Agricultural practices and biodiversity: Conservation policies for semi-natural grasslands in europe. *Current Biology* **34**, R753–R761 (2024).

9. R. C. Lacy, Loss of Genetic Diversity from Managed Populations: Interacting Effects of Drift, Mutation, Immigration, Selection, and Population Subdivision. *Conservation Biology* **1**, 143–158 (1987).

10. R. Lande, Mutation and Conservation. *Conservation Biology* **9**, 782–791 (1995).

11. R. Lande, S. Shannon, The Role of Genetic Variation in Adaptation and Population Persistence in a Changing Environment. *Evolution* **50**, 434–437 (1996).

12. G. Bertorelle, *et al.*, Genetic load: genomic estimates and applications in non-model animals. *Nature Reviews Genetics* **23**, 492–503 (2022).

13. M. Lynch, J. Conery, R. Burger, Mutation accumulation and the extinction of small populations. *The American Naturalist* **146**, 489–518 (1995).

14. J. F. Crow, Some possibilities for measuring selection intensities in man. *Human Biology* **30**, 1–13 (1958).

15. M. Lynch, W. Gabriel, Mutation Load and the Survival of Small Populations. *Evolution* **44**, 1725–1737 (1990).

16. D. L. Gilroy, K. P. Phillips, D. S. Richardson, C. van Oosterhout, Toll-like receptor variation in the bottlenecked population of the Seychelles warbler: computer simulations see the 'ghost of selection past' and quantify the 'drift debt'. *Journal of Evolutionary Biology* **30**, 1276–1287 (2017).

17. A. V. Pinto, B. Hansson, I. Patramanis, H. E. Morales, C. van Oosterhout, The impact of habitat loss and population fragmentation on genomic erosion. *Conservation Genetics* **25**, 49–57 (2024).

18. H. A. Jackson, *et al.*, Genomic erosion in a demographically recovered bird species during conservation rescue. *Conservation Biology* **36**, e13918 (2022).

19. M. Dehasque, *et al.*, Temporal dynamics of woolly mammoth genome erosion prior to extinction. *Cell* **187**, 3531–3540.e13 (2024).

20. A. Andersson, S. Karlsson, N. Ryman, L. Laikre, Monitoring genetic diversity with new indicators applied to an alpine freshwater top predator. *Molecular Ecology* **31**, 6422–6439 (2022).

21. D. O'Brien, *et al.*, Bringing together approaches to reporting on within species genetic diversity. *Journal of Applied Ecology* **59**, 2227–2233 (2022).

22. K. Theissinger, *et al.*, How genomics can help biodiversity conservation. *Trends in Genetics* **39**, 545–559 (2023).

23. D. Díez-del-Molino, F. Sánchez-Barreiro, I. Barnes, M. T. P. Gilbert, L. Dalén, Quantifying temporal genomic erosion in endangered species. *Trends in Ecology & Evolution* **33**, 176–185 (2018).

24. H. Ellegren, N. Galtier, Determinants of genetic diversity. *Nature Reviews Genetics* **17**, 422–433 (2016).

25. J. Romiguier, *et al.*, Comparative population genomics in animals uncovers the determinants of genetic diversity. *Nature* **515**, 261–263 (2014).

26. A. Mackintosh, *et al.*, The determinants of genetic diversity in butterflies. *Nature Communications* **10**, 3466 (2019).

27. G. Hewitt, The genetic legacy of the Quaternary ice ages. *Nature* **405**, 907–913 (2000).

28. J. A. Robinson, *et al.*, Genomic flatlining in the endangered island fox. *Current Biology* **26**, 1183–1189 (2016).

29. J. A. Robinson, *et al.*, The critically endangered vaquita is not doomed to extinction by inbreeding depression. *Science* **376**, 635–639 (2022).

30. M. F. DiLeo, A. Nair, M. Kardos, A. Husby, M. Saastamoinen, Demography and environment modulate the effects of genetic diversity on extinction risk in a butterfly metapopulation. *Proceedings of the National Academy of Sciences* **121**, e2309455121 (2024).

31. J. C. Teixeira, C. D. Huber, The inflated significance of neutral genetic diversity in conservation genetics. *Proceedings of the National Academy of Sciences* **118**, e2015096118 (2021).

32. A. García-Dorado, A. Caballero, Neutral genetic diversity as a useful tool for conservation biology. *Conservation Genetics* **22**, 541–545 (2021).

33. M. Kardos, H. R. Taylor, H. Ellegren, G. Luikart, F. W. Allendorf, Genomics advances the study of inbreeding depression in the wild. *Evolutionary Applications* **9**, 1205–1218 (2016).

34. M. K. Schwartz, G. Luikart, R. S. Waples, Genetic monitoring as a promising tool for conservation and management. *Trends in Ecology & Evolution* **22**, 25–33 (2007).

35. S. Hoban, *et al.*, Effective population size remains a suitable, pragmatic indicator of genetic diversity for all species, including forest trees. *Biological Conservation* **253**, 108906 (2021).

36. M. Kardos, *et al.*, The crucial role of genome-wide genetic variation in conservation. *Proceedings of the National Academy of Sciences* **118**, e2104642118 (2021).

37. N. Dussex, H. E. Morales, C. Grossen, L. Dalén, C. van Oosterhout, Purging and accumulation of genetic load in conservation. *Trends in Ecology & Evolution* **38**, 961–969 (2023).

38. C. van Oosterhout, Mutation load is the spectre of species conservation. *Nature Ecology & Evolution* **4**, 1004–1006 (2020).

39. T. van der Valk, D. Díez-del-Molino, T. Marques-Bonet, K. Guschanski, L. Dalén, Historical Genomes Reveal the Genomic Consequences of Recent Population Decline in Eastern Gorillas. *Current Biology* **29**, 165–170.e6 (2019).

40. J. von Seth, *et al.*, Genomic insights into the conservation status of the world's last remaining Sumatran rhinoceros populations. *Nature Communications* **12**, 2393 (2021).

41. G. Femerling, *et al.*, Genetic Load and Adaptive Potential of a Recovered Avian Species that Narrowly Avoided Extinction. *Molecular Biology and Evolution* **40**, msad256 (2023).

42. M. Ihse, Swedish agricultural landscapes patterns and changes during the last 50 years, studied by aerial photos. *Landscape and Urban Planning* **31**, 21–37 (1995).

43. R. Lindborg, O. Eriksson, Historical Landscape Connectivity Affects Present Plant Species Diversity. *Ecology* **85**, 1840–1845 (2004).

44. D. L. Wagner, R. Fox, D. M. Salcido, L. A. Dyer, A window to the world of global insect declines: Moth biodiversity trends are complex and heterogeneous. *Proceedings of the National Academy of Sciences* **118**, e2002549117 (2021).

45. M. S. Warren, *et al.*, The decline of butterflies in europe: Problems, significance, and possible solutions. *Proceedings of the National Academy of Sciences* **118**, e2002551117 (2021).

46. J. C. Habel, *et al.*, Butterfly community shifts over two centuries. *Conservation Biology* **30**, 754–762 (2016).

47. SLU Artdatabanken, *Rödlistade arter i Sverige 2020* (SLU, 2020).

48. C. Fägerström, Lund University Biological Museum - Insect collections Inventory. (2024). https://doi.org/10.15468/dahk2a.

49. Z. J. Nolen, M. Rundlöf, A. Runemark, Species-specific erosion of genetic diversity in grassland butterflies depends on landscape land cover. *Biological Conservation* **296**, 110694 (2024).

50. M. T. P. Gilbert, *et al.*, Recharacterization of ancient DNA miscoding lesions: Insights in the era of sequencing-by-synthesis. *Nucleic Acids Research* **35**, 1–10 (2007).

51. M. Stiller, *et al.*, Patterns of nucleotide misincorporations during enzymatic amplification and direct large-scale sequencing of ancient DNA. *Proceedings of the National Academy of Sciences* **103**, 13578–13584 (2006).

52. P. W. Hedrick, *Genetics of Populations* (Jones & Bartlett Publishers, 2009).

53. R. McQuillan, *et al.*, Runs of homozygosity in european populations. *The American Journal of Human Genetics* **83**, 359–372 (2008).

54. E. A. Thompson, Identity by descent: Variation in meiosis, across genomes, and in populations. *Genetics* **194**, 301–326 (2013).

55. S. Glémin, How are deleterious mutations purged? Drift versus nonrandom mating. *Evolution* **57**, 2678–2687 (2003).

56. M. Kirkpatrick, P. Jarne, The effects of a bottleneck on inbreeding depression and the genetic load. *The American Naturalist* **155**, 154–167 (2000).

57. J. Wang, W. G. Hill, D. Charlesworth, B. Charlesworth, Dynamics of inbreeding depression due to deleterious mutations in small populations: mutation parameters and inbreeding rate. *Genetics Research* **74**, 165–178 (1999).

58. B. Charlesworth, Mutational load, inbreeding depression and heterosis in subdivided populations. *Molecular Ecology* **27**, 4991–5003 (2018).

59. D. Kleinman-Ruiz, *et al.*, Purging of deleterious burden in the endangered iberian lynx. *Proceedings of the National Academy of Sciences* **119**, e2110614119 (2022).

60. E. Humble, *et al.*, Conservation management strategy impacts inbreeding and mutation load in scimitar-horned oryx. *Proceedings of the National Academy of Sciences* **120**, e2210756120 (2023).

61. K. Johannesson, L. Laikre, Monitoring of genetic diversity in environmental monitoring [in Swedish]. *Report to the Swedish Agency for Marine and Water Management (dnr. HaV 3642-2018, 3643-2018)* (2020).

62. R. Lande, Neutral Theory of Quantitative Genetic Variance in an Island Model with Local Extinction and Colonization. *Evolution* **46**, 381–389 (1992).

63. M. Nei, N. Takahata, Effective population size, genetic diversity, and coalescence time in subdivided populations. *Journal of Molecular Evolution* **37**, 240–244 (1993).

64. Z. Gompert, A. Springer, M. Brady, S. Chaturvedi, L. K. Lucas, Genomic time-series data show that gene flow maintains high genetic diversity despite substantial genetic drift in a butterfly species. *Molecular Ecology* **30**, 4991–5008 (2021).

65. P. W. Hedrick, J. R. Adams, J. A. Vucetich, Reevaluating and Broadening the Definition of Genetic Rescue. *Conservation Biology* **25**, 1069–1070 (2011).

66. P. W. Hedrick, A. Garcia-Dorado, Understanding inbreeding depression, purging, and genetic rescue. *Trends in Ecology & Evolution* **31**, 940–952 (2016).

67. D. A. Bell, *et al.*, The Exciting Potential and Remaining Uncertainties of Genetic Rescue. *Trends in Ecology & Evolution* **34**, 1070–1079 (2019).

68. E. L. Landguth, *et al.*, Quantifying the lag time to detect barriers in landscape genetics. *Molecular Ecology* **19**, 4179–4191 (2010).

69. C. W. Epps, N. Keyghobadi, Landscape genetics in a changing world: disentangling historical and contemporary influences and inferring change. *Molecular Ecology* **24**, 6021–6040 (2015).

70. Y. B. Simons, G. Sella, The impact of recent population history on the deleterious mutation load in humans and close evolutionary relatives. *Current Opinion in Genetics & Development* **41**, 150–158 (2016).

71. Y. Xue, *et al.*, Mountain gorilla genomes reveal the impact of long-term population decline and inbreeding. *Science* **348**, 242–245 (2015).

72. C. Grossen, F. Guillaume, L. F. Keller, D. Croll, Purging of highly deleterious mutations through severe bottlenecks in Alpine ibex. *Nature Communications* **11**, 1001 (2020).

73. N. Dussex, *et al.*, Population genomics of the critically endangered kākāpō. *Cell Genomics* **1**, 100002 (2021).

74. A. Khan, *et al.*, Genomic evidence for inbreeding depression and purging of deleterious genetic variation in indian tigers. *Proceedings of the National Academy of Sciences* **118**, e2023018118 (2021).

75. B. Charlesworth, Evidence against Fisher's theory of dominance. *Nature* **278**, 848–849 (1979).

76. F. Manna, G. Martin, T. Lenormand, Fitness landscapes: An alternative theory for the dominance of mutation. *Genetics* **189**, 923–937 (2011).

77. A. García-Dorado, A. Caballero, On the average coefficient of dominance of deleterious spontaneous mutations. *Genetics* **155**, 1991–2001 (2000).

78. C. D. Huber, A. Durvasula, A. M. Hancock, K. E. Lohmueller, Gene expression drives the evolution of dominance. *Nature Communications* **9**, 2750 (2018).

79. B. Charlesworth, D. Charlesworth, *Elements of evolutionary genetics* (Roberts; Company, 2010).

80. L. F. Keller, D. M. Waller, Inbreeding effects in wild populations. *Trends in Ecology & Evolution* **17**, 230–241 (2002).

81. D. Charlesworth, J. H. Willis, The genetics of inbreeding depression. *Nature Reviews Genetics* **10**, 783–796 (2009).

82. G. M. Cooper, *et al.*, Distribution and intensity of constraint in mammalian genomic sequence. *Genome Research* **15**, 901–913 (2005).

83. C. D. Huber, B. Y. Kim, K. E. Lohmueller, Population genetic models of GERP scores suggest pervasive turnover of constrained sites across mammalian evolution. *PLOS Genetics* **16**, e1008827 (2020).

84. C. C. Kyriazis, J. A. Robinson, K. E. Lohmueller, Using computational simulations to model deleterious variation and genetic load in natural populations. *The American Naturalist* **202**, 737–752 (2023).

85. C. Bortoluzzi, *et al.*, Lepidoptera genomics based on 88 chromosomal reference sequences informs population genetic parameters for conservation. *bioRxiv* (2023). https://doi.org/10.1101/2023.04.14.536868.

86. R. Frankham, Genetic rescue of small inbred populations: meta-analysis reveals large and consistent benefits of gene flow. *Molecular Ecology* **24**, 2610–2618 (2015).

87. K. Ralls, P. Sunnucks, R. C. Lacy, R. Frankham, Genetic rescue: A critique of the evidence supports maximizing genetic diversity rather than minimizing the introduction of putatively harmful genetic variation. *Biological Conservation* **251**, 108784 (2020).

88. A. L. K. Mattila, *et al.*, High genetic load in an old isolated butterfly population. *Proceedings of the National Academy of Sciences* **109**, E2496–E2505 (2012).

89. I. Saccheri, *et al.*, Inbreeding and extinction in a butterfly metapopulation. *Nature* **392**, 491–494 (1998).

90. L. B. Pettersson, H. Arnberg, *Svensk dagfjärilsövervakning, årsrapport för 2023* (Biologiska institutionen, Lunds universitet, 2024).

91. S. Hoban, *et al.*, Genetic diversity targets and indicators in the CBD post-2020 Global Biodiversity Framework must be improved. *Biological Conservation* **248**, 108654 (2020).

92. L. Laikre, *et al.*, Post-2020 goals overlook genetic diversity. *Science* **367**, 1083–1085 (2020).

93. A. Brüniche-Olsen, K. F. Kellner, C. J. Anderson, J. A. DeWoody, Runs of homozygosity have utility in mammalian conservation and evolutionary studies. *Conservation Genetics* **19**, 1295–1307 (2018).

94. G. Formenti, *et al.*, The era of reference genomes in conservation genomics. *Trends in Ecology & Evolution* **37**, 197–202 (2022).

95. V. G. Twort, J. Minet, C. W. Wheat, N. Wahlberg, Museomics of a rare taxon: placing Whalleyanidae in the Lepidoptera Tree of Life. *Systematic Entomology* **46**, 926–937 (2021).

96. F. Mölder, *et al.*, Sustainable data analysis with snakemake [version 2; peer review: 2 approved]. *F1000Research* **10** (2021).

97. Z. J. Nolen, Zjnolen/PopGLen: V0.3.0. (2024). https://doi.org/10.5281/zenodo.13785563. Deposited September 2024.

98. S. Chen, Y. Zhou, Y. Chen, J. Gu, Fastp: An ultra-fast all-in-one FASTQ preprocessor. *Bioinformatics* **34**, i884–i890 (2018).

99. H. Li, R. Durbin, Fast and accurate long-read alignment with BurrowsWheeler transform. *Bioinformatics* **26**, 589–595 (2010).

100. R. Martiniano, E. Garrison, E. R. Jones, A. Manica, R. Durbin, Removing reference bias and improving indel calling in ancient DNA data analysis by mapping to a sequence variation graph. *Genome Biology* **21**, 250 (2020).

101. K. Lohse, R. Vila, The genome sequence of the common blue, *Polyommatus icarus* (rottemburg, 1775) [version 1; peer review: 1 approved]. *Wellcome Open Research* **8** (2023).

102. K. Lohse, *et al.*, The genome sequence of the mazarine blue, *Cyaniris semiargus* (rottemburg, 1775) [version 1; peer review: 1 approved]. *Wellcome Open Research* **8** (2023).

103. A. Hayward, K. Lohse, D. R. Laetsch, R. Vila, E. Taluy, The genome sequence of the silver-studded blue, *Plebejus argus* (linnaeus, 1758) [version 1; peer review: 2 approved]. *Wellcome Open Research* **7** (2022).

104. H. Li, Aligning sequence reads, clone sequences and assembly contigs with BWA-MEM. (2013). https://doi.org/10.48550/arXiv.1303.3997.

105. Picard toolkit. *Broad Institute, GitHub Repository* (2019). Deposited 2019.

106. G. A. van der Auwera, B. D. O'Connor, *Genomics in the Cloud: Using Docker, GATK, and WDL in Terra* (O'Reilly Media, Inc., 2020).

107. P. Danecek, *et al.*, Twelve years of SAMtools and BCFtools. *GigaScience* **10** (2021).

108. E. Garrison, *et al.*, Variation graph toolkit improves read mapping by representing genetic variation in the reference. *Nature Biotechnology* **36**, 875–879 (2018).

109. A. Peltzer, *et al.*, EAGER: efficient ancient genome reconstruction. *Genome Biology* **17**, 1–14 (2016).

110. G. Jun, M. K. Wing, G. R. Abecasis, H. M. Kang, An efficient and scalable analysis framework for variant extraction and refinement from population-scale DNA sequence data. *Genome Research* **25**, 918–925 (2015).

111. J. Neukamm, A. Peltzer, K. Nieselt, DamageProfiler: Fast damage pattern calculation for ancient DNA. *Bioinformatics* **37**, 3652–3653 (2021).

112. K. L. Korunes, K. Samuk, pixy: Unbiased estimation of nucleotide diversity and divergence in the presence of missing data. *Molecular Ecology Resources* **21**, 1359–1368 (2021).

113. R. R. Hudson, M. Slatkin, W. P. Maddison, Estimation of levels of gene flow from DNA sequence data. *Genetics* **132**, 583–589 (1992).

114. G. Bhatia, N. Patterson, S. Sankararaman, A. L. Price, Estimating and interpreting FST: The impact of rare variants. *Genome Research* **23**, 1514–1521 (2013).

115. R. K. Waples, A. Albrechtsen, I. Moltke, Allele frequency-free inference of close familial relationships from genotypes or low-depth sequencing data. *Molecular Ecology* **28**, 35–48 (2019).

116. K. Hanghøj, I. Moltke, P. A. Andersen, A. Manica, T. S. Korneliussen, Fast and accurate relatedness estimation from high-throughput sequencing data in the presence of inbreeding. *GigaScience* **8**, giz034 (2019).

117. A. Manichaikul, *et al.*, Robust relationship inference in genome-wide association studies. *Bioinformatics* **26**, 2867–2873 (2010).

118. T. S. Korneliussen, A. Albrechtsen, R. Nielsen, ANGSD: Analysis of Next Generation Sequencing Data. *BMC Bioinformatics* **15**, 1–13 (2014).

119. J. Meisner, A. Albrechtsen, Inferring population structure and admixture proportions in low-depth NGS data. *Genetics* **210**, 719–731 (2018).

120. E. A. Fox, A. E. Wright, M. Fumagalli, F. G. Vieira, ngsLD: Evaluating linkage disequilibrium using genotype likelihoods. *Bioinformatics* **35**, 3855–3856 (2019).

121. L. Skotte, T. S. Korneliussen, A. Albrechtsen, Estimating individual admixture proportions from next generation sequencing data. *Genetics* **195**, 693–702 (2013).

122. P. Pečnerová, *et al.*, High genetic diversity and low differentiation reflect the ecological versatility of the African leopard. *Current Biology* **31**, 1862–1871.e5 (2021).

123. G. Garcia-Erill, A. Albrechtsen, Evaluation of model fit of inferred admixture proportions. *Molecular Ecology Resources* **20**, 936–949 (2020).

124. V. Narasimhan, *et al.*, BCFtools/RoH: A hidden markov model approach for detecting autozygosity from next-generation sequencing data. *Bioinformatics* **32**, 1749–1751 (2016).

125. E. Santiago, *et al.*, Recent demographic history inferred by high-resolution analysis of linkage disequilibrium. *Molecular Biology and Evolution* **37**, 3642–3653 (2020).

126. I. Novo, *et al.*, Impact of population structure in the estimation of recent historical effective population size by the software GONE. *Genetics Selection Evolution* **55**, 86 (2023).

127. M. Petr, B. C. Haller, P. L. Ralph, F. Racimo, *slendr*: a framework for spatio-temporal population genomic simulations on geographic landscapes. *Peer Community Journal* **3** (2023).

128. F. Baumdicker, *et al.*, Efficient ancestry and mutation simulation with msprime 1.0. *Genetics* **220**, iyab229 (2022).

129. P. D. Keightley, *et al.*, Estimation of the spontaneous mutation rate in heliconius melpomene. *Molecular Biology and Evolution* **32**, 239–243 (2015).

130. W. McLaren, *et al.*, The Ensembl Variant Effect Predictor. *Genome Biology* **17**, 122 (2016).

131. E. V. Davydov, *et al.*, Identifying a High Fraction of the Human Genome to be under Selective Constraint Using GERP++. *PLOS Computational Biology* **6**, e1001025 (2010).

132. V. E. Kutschera, *et al.*, GenErode: a bioinformatics pipeline to investigate genome erosion in endangered and extinct species. *BMC Bioinformatics* **23**, 1–17 (2022).

133. K. Lohse, D. Laetsch, R. Vila, The genome sequence of the small copper, *Lycaena phlaeas* (linnaeus, 1760) [version 1; peer review: 2 approved with reservations]. *Wellcome Open Research* **6** (2021).

134. A. Hayward, C. Wright, The genome sequence of the holly blue, *Celastrina argiolus* (linnaeus, 1758) [version 1; peer review: 2 approved]. *Wellcome Open Research* **6** (2021).

135. J. Hinojosa Galisteo, R. Vila, The genome sequence of the green-underside blue, *Glaucopsyche alexis* (poda, 1761) [version 1; peer review: 2 approved]. *Wellcome Open Research* **6** (2021).

136. K. Lohse, A. Hayward, R. Vila, C. Howe, The genome sequence of the adonis blue, *Lysandra bellargus* (rottemburg, 1775) [version 1; peer review: 2 approved, 2 approved with reservations]. *Wellcome Open Research* **7** (2022).

137. S. Kumar, *et al.*, TimeTree 5: An expanded resource for species divergence times. *Molecular Biology and Evolution* **39**, msac174 (2022).

Figures

Figure 1. Sampling design and changes in genetic diversity, differentiation, and inbreeding in the focal species. (A) Images of the three focal species. (B) Map of the sampling area in southern Sweden, sampling locations are approximate. Circles represent areas with modern samples in at least one of the species and triangles represent areas with historical samples, see Table S1 for complete sampling information. (C) Change in individual heterozygosity over time, measured as heterozygous sites per 1000bp, excluding transitions. Each point represents an individual sample, grouped into historical and modern samples per species. Coloring refers to sampling region and corresponds to the map in panel B. (D) Change in inbreeding coefficients over time, estimated using runs of homozygosity larger than 100kb (F_{RoH}). (E) Change in pairwise population genetic differentiation, F_{ST} over time between equivalent comparisons in each time period. Color of the points and line refer to the geographic distance between populations. Populations with no connecting line refer to pairs of modern sample populations that have no comparable historic pair. In C & D, results of linear mixed models assessing the effect of time period on the response are shown using the following scale, where panels without * are not significant (P > 0.05): * P <= 0.05, ** P <= 0.01, *** P <= 0.001.

Figure 2. Population structure of the focal species. (A) Principal Component Analysis (PCA) of the three focal species. Shapes refer to sampling period, with each circle representing a modern and each triangle a historical individual, with colors corresponding to the sampling locations in Figure 1B. Percentages on each axis refer to the proportion of total variance explained by the component. (B) Admixture analyses for the three focal species. Each color represents one of K genetic clusters, with bars representing individuals, colored by their probability of belonging to a given cluster. For *Po. icarus* and *Pl. argus*, the best fit was at K = 1, but K = 2 is shown for illustrative purposes. For *Cy. semiargus*, the best fit K = 5 is shown.

Figure 3. Temporal changes in deleterious burden in the focal species (A) Individual inbreeding coefficients (F_{RoH}) partitioned by *RoH* size class. Longer *RoH* indicate more recent common ancestry of the identical haplotypes. (B) Estimates of total deleterious mutation burden for each individual of the three focal species across three categories of putatively deleterious mutations: I) missense (i.e. weakly deleterious; upper), II) loss of function (LoF, i.e. strongly deleterious; middle), and III) conserved positions (presumed strongly deleterious; lower). Total burden is estimated per individual as the total count of derived alleles of a given mutation category per 1000 called genotypes. C) Homozygous deleterious mutation burden for the same mutation categories as in B, but only calculated using homozygous derived positions in the numerator. In B & C, results of linear mixed models with burden as a response to time period are shown in each panel, where panels without * are not significant (P > 0.05): * P <= 0.05, ** P <= 0.01, *** P <= 0.001.

867

Figure 4. Changes in heterozygosity projected over 100 years based on the rate of change estimated from modern and historical samples for each of 8 species. Species are grouped by conservation status, which follows the species name on the x-axis. Background coloration refers to the three genetic decline thresholds outlined by Andersson et al (20), where a retention of >=95% over 100 year is considered 'acceptable' (green), a retention of 75-94% as 'warning' (yellow), and a retention of <75% as 'alarm' (red). Points represent median estimates for change in heterozygosity across all historical/modern individual pairs for a species. Species with bars have more than one possible sample pair, with error bars illustrating the spread of estimates across all sample pairs. **Sc. orion* and *Pl. argyrognomon* include pinned museum specimens for both the modern and historical individuals. *Pl. argyrognomon* is additionally is the only species aligned to a non species-specific reference (Table S12).

868

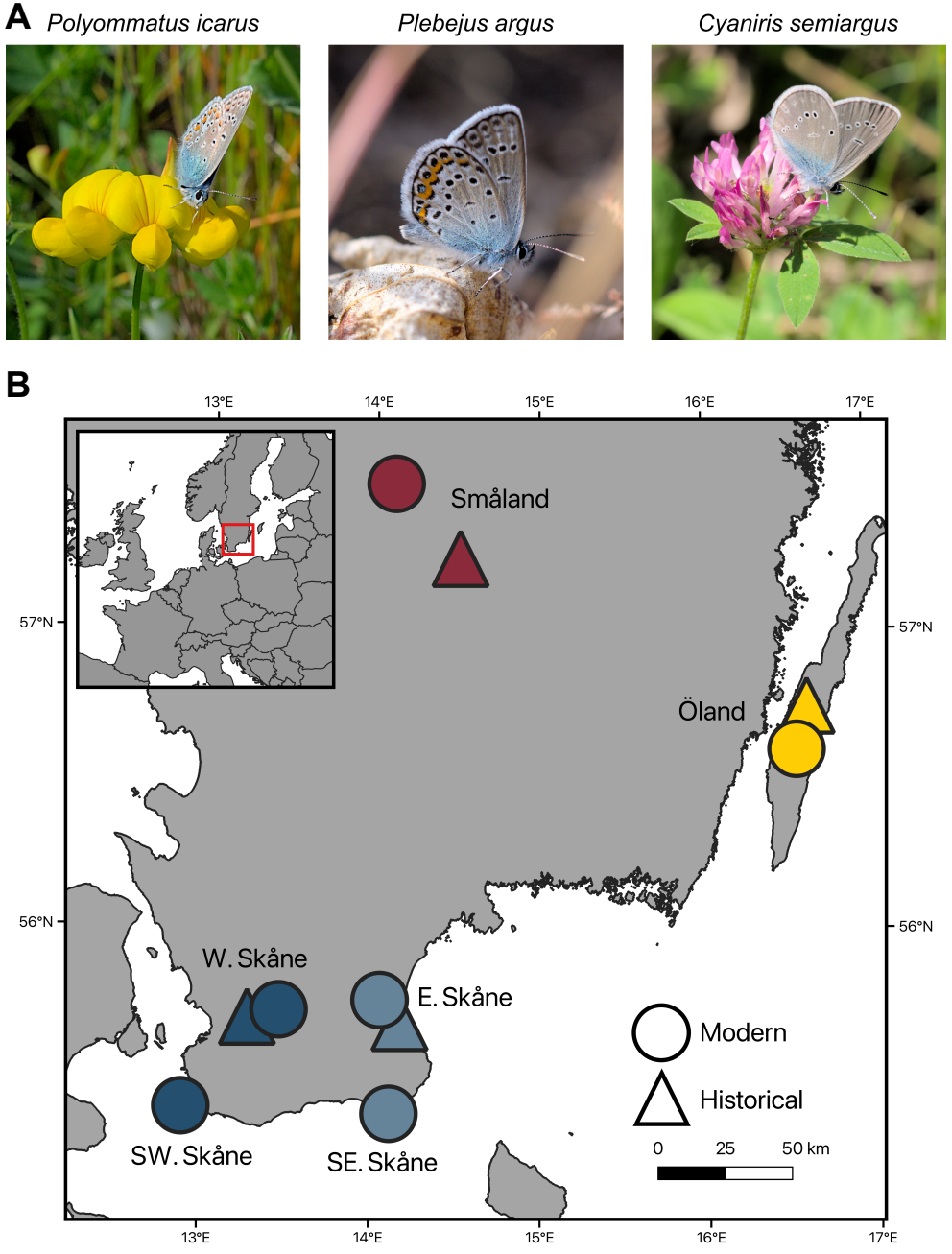
A
Polyommatus icarus
Plebejus argus
Cyaniris semiargus
B
13°E
14°E
15°E
16°E
17°E
57°N
56°N
Småland
Öland
W. Skåne
E. Skåne
SW. Skåne
SE. Skåne
Modern
Historical
0
25
50 km
C
Po. icarus
Pl. argus
Cy. semiargus
Heterozygous sites per 1000bp
(excl. transitions)
4.0
3.5
3.0
2.5
2.0
1.5
**
Historical
Modern
D
F_{RoH} (RoH > 100kb)
0.4
0.3
0.2
0.1
0.0
E
Hudson F_{ST}
0.12
0.10
0.08
0.05
0.02
Distance (km)
250
200
150
100
50

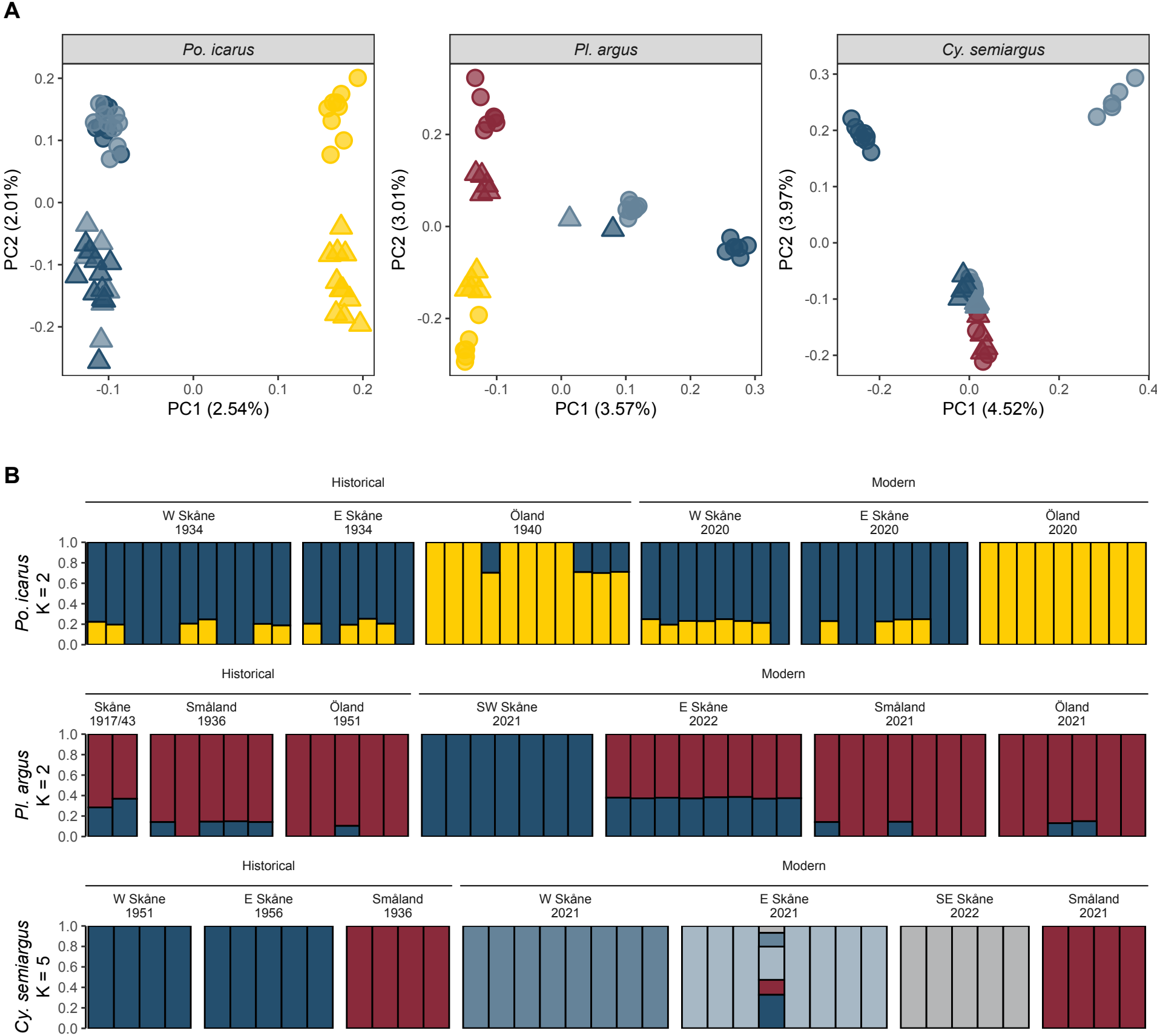
A
Po. icarus
Pl. argus
Cy. semiargus
PC2 (2.01%)
PC1 (2.54%)
PC2 (3.01%)
PC1 (3.57%)
PC2 (3.97%)
PC1 (4.52%)
B
Historical
Modern
W Skåne 1934
E Skåne 1934
Öland 1940
W Skåne 2020
E Skåne 2020
Öland 2020
Po. icarus K = 2
Skåne 1917/43
Småland 1936
Öland 1951
SW Skåne 2021
E Skåne 2022
Småland 2021
Öland 2021
Pl. argus K = 2
W Skåne 1951
E Skåne 1956
Småland 1936
W Skåne 2021
E Skåne 2021
SE Skåne 2022
Småland 2021
Cy. semiargus K = 5

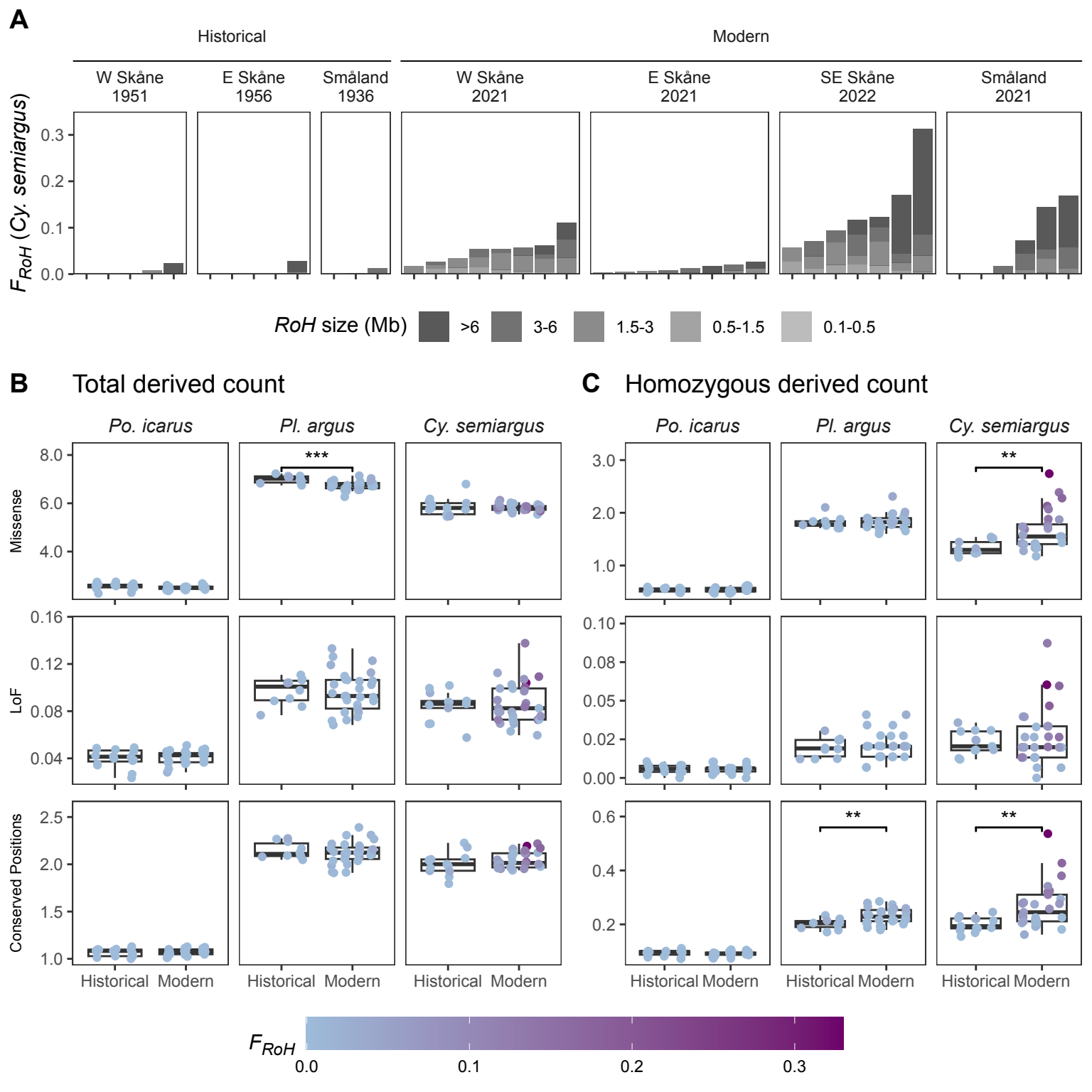
A
Historical
Modern
W Skåne 1951
E Skåne 1956
Småland 1936
W Skåne 2021
E Skåne 2021
SE Skåne 2022
Småland 2021
F_{RoH} (Cy. semiargus)
0.0
0.1
0.2
0.3
RoH size (Mb)
>6
3-6
1.5-3
0.5-1.5
0.1-0.5
B Total derived count
C Homozygous derived count
Po. icarus
Pl. argus
Cy. semiargus
Missense
LoF
Conserved Positions
***
**
Historical
Modern
F_{RoH}
0.0
0.1
0.2
0.3

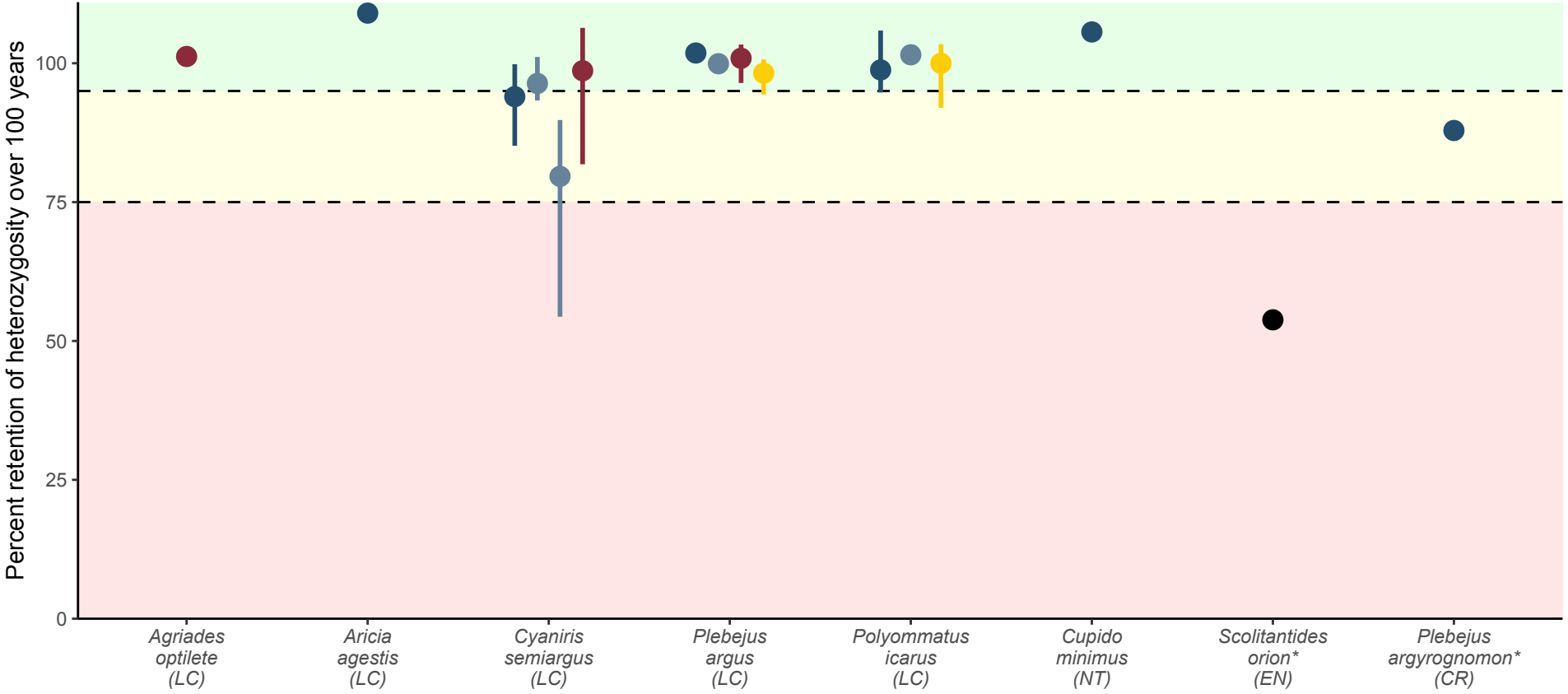
Percent retention of heterozygosity over 100 years
100
75
50
25
0
Agriades optilete (LC)
Aricia agestis (LC)
Cyaniris semiargus (LC)
Plebejus argus (LC)
Polyommatus icarus (LC)
Cupido minimus (NT)
Scolitantides orion* (EN)
Plebejus argyrognomon* (CR)